Unstable dimension variability in coupled chaotic systems

Ying-Cheng Lai,[1,2,*] David Lerner,[1] Kaj Williams,[1] and Celso Grebogi[3]
[1]*Department of Mathematics, University of Kansas, Lawrence, Kansas 66045*
[2]*Department of Physics and Astronomy, University of Kansas, Lawrence, Kansas 66045*
[3]*Institute for Plasma Research, Department of Mathematics, Institute for Physical Science and Technology, University of Maryland, College Park, Maryland 20742*
(Received 7 May 1999)

Systems of coupled chaotic maps and flows arise in many situations of physical and biological interest. The aim of this paper is to analyze and to present numerical evidence for a common type of nonhyperbolic behavior in these systems: unstable dimension variability. We show that unstable periodic orbits embedded in the dynamical invariant set of such a system can typically have different numbers of unstable directions. The consequence of this may be severe: the system cannot be modeled deterministically in the sense that no trajectory of the model can be realized by the natural chaotic system that the model is supposed to describe and quantify. We argue that unstable dimension variability can arise for small values of the coupling parameter. Severe modeling difficulties, nonetheless, occur only for reasonable coupling when the unstable dimension variability is appreciable. We speculate about the possible physical consequences in this case. [S1063-651X(99)09711-1]

PACS number(s): 05.45.Jn, 0.5.45.Pq

I. INTRODUCTION

Coupled dynamical systems are relevant to a large variety of physical and biological phenomena [1]. Arrays of Josephson junctions [2] and coupled solid lasers [3] are well known examples in physics. In biology, vital organs such as the heart and the auditory, visual, and central nervous systems are complex networks of many small elements such as cells and neurons. Typically, the collective behavior of all the units in the network can be extremely rich, ranging from steady state or periodic oscillations to chaotic or turbulent motion.

For the study and understanding of such behavior, it is desirable to model the networks in the Newtonian sense. But do such models make any sense if elements in the network are chaotic? Assume that one has a mathematically exact model of a system of N coupled maps or flows, written both in discrete and continuous time, respectively, as follows:

$$\mathbf{x}_{n+1}^{i}=\mathbf{F}(\mathbf{x}_{n}^{i})-\frac{\epsilon}{2}\sum_{j=1}^{N}G_{ij}\mathbf{H}(\mathbf{x}_{n}^{j}),\quad i=1,\ldots,N, \tag{1}$$

$$\frac{d\mathbf{x}^{i}}{dt}=\mathbf{F}(\mathbf{x}^{i})-\frac{\epsilon}{2}\sum_{j=1}^{N}G_{ij}\mathbf{H}(\mathbf{x}^{j}),\quad i=1,\ldots,N, \tag{2}$$

where $\mathbf{x}_i\in\mathbf{R}^m$ is an m-dimensional vector, ϵ is a parameter characterizing the coupling strength, and $\mathbf{H}(\mathbf{x})$ is a smooth function. The synchronization manifold $\mathcal{M}$ of the network is defined by $\mathbf{x}^1=\mathbf{x}^2=\cdots=\mathbf{x}^N$. In a situation expected to arise frequently in physical and biological networks, the elements G_{ij} of the coupling matrix satisfy the condition $\Sigma_j G_{ij}=0$ for all i. If, in the absence of noise, an orbit of the system starts from an initial condition in $\mathcal{M}$ and evolves according to Eq. (1) or Eq. (2), then the orbit remains synchronized (i.e., in $\mathcal{M}$) for all time. The synchronization manifold is thus an *invariant* manifold of the system.

When the dynamics of each individual element in the system is chaotic in the absence of coupling, as the coupling strength ϵ increases, the elements may or may not become synchronized depending on the transverse stability of $\mathcal{M}$. A number of recent papers have examined various aspects of the stability of the synchronization manifold for coupled chaotic systems [4]. In this paper, we wish to address the extent to which a real system of coupled chaotic maps or flows, differing slightly from a mathematical model due to modeling errors, can be modeled by systems such as the ones described by either Eq. (1) or Eq. (2).

Our principal result is that there are wide parameter regimes for which these models do not accurately represent the deterministic evolution of the real systems. Specifically, suppose one constructs a system of coupled chaotic maps or flows in a laboratory, which is as close as possible to being described by either of the above equations, and one records an experimental time series $\mathbf{x}(t)$. Then *no* trajectories of the mathematical model will remain close to the measured trajectory $\mathbf{x}(t)$ for appreciable lengths of time. We say in this case that there is no model shadowability [5]. Thus, one should be extremely careful when interpreting results from models of coupled chaotic elements such as these represented by Eq. (1) or Eq. (2). Often, in such cases, the only results that can be trusted are statistical invariants obtained from a large number of trajectories of the model [6]. One important implication is that in laboratory or industrial experiments involving a system of coupled chaotic oscillators, it may be more advantageous to work directly with the experimentally measured time series rather than with the mathematical model when attempting to analyze the system, even if the physical assumptions employed in the construction of

*Present address: Department of Mathematics, Arizona State University, Tempe, AZ 85287-1804.

the model are considered reasonable and as accurate as possible. The actual solution of the real system resides, in this case, in the time-series data.

The above strong conclusions are a consequence of the recently documented phenomenon known as *unstable dimension variability*, a type of nonhyperbolicity that is believed to arise commonly in high-dimensional chaotic systems [7,8]. Roughly, unstable-dimension variability means that different unstable periodic orbits, which are thought to be dense on the chaotic attractor, have different numbers of unstable directions. So, on a typical chaotic orbit, there is no continuous decomposition of the tangent space at each trajectory point into stable and unstable subspaces, violating one of the basic requirements for hyperbolicity [9].

The main goal of this paper is then to establish the existence of unstable dimension variability for systems of coupled chaotic maps or flows such as those described by Eq. (1) or Eq. (2). Specifically, we will present theoretical arguments and explicit numerical evidence that unstable dimension variability in Eq. (1) occurs for small coupling among the elements in the network. Usually, it is extremely difficult to analyze and even to numerically compute unstable periodic orbits for Eq. (1). However, since the synchronization manifold $\mathcal{M}$ is invariant, a typical trajectory in the chaotic attractor in $\mathcal{M}$ is also a trajectory of the full system Eq. (1). Therefore, for low-dimensional chaotic attractors in $\mathcal{M}$, such as those arising in two-dimensional invertible maps or three-dimensional flows, it is possible to enumerate the periodic orbits embedded in the attractor and to analyze their stabilities. For this purpose, we choose the coupled Hénon map lattice for which unstable periodic orbits of reasonably high periods in the synchronization manifold $\mathcal{M}$ can be computed explicitly. Our investigation shows that these periodic orbits exhibit unstable dimension variability. Although we present our computational results using the Hénon map lattice, the argument for unstable dimension variability is general and our conclusions should hold for any coupled chaotic system with an invariant synchronization manifold. A preliminary version of part of this material has recently appeared [10].

The remainder of this paper is organized as follows. In Sec. II, we describe the relationship between unstable dimension variability and modeling shadowability, and we give a general argument that unstable dimension variability arises commonly in systems of coupled chaotic oscillators. In Sec. III, we study an illustrative example: the system of two diffusively coupled Hénon maps [11] for which unstable dimension variability can be explicitly demonstrated by a systematic computation of unstable periodic orbits and their transverse stabilities. In Sec. IV, we consider systems of N ($N>2$) diffusively coupled Hénon maps and give theoretical and numerical analyses for unstable dimension variability. In Sec. V, we address the issue of generic orbits. In Sec. VI, we discuss our results and offer some speculation.

II. UNSTABLE DIMENSION VARIABILITY IN SYSTEMS OF COUPLED CHAOTIC OSCILLATORS

Generally, a necessary requirement for a model is robustness under small perturbations. One can easily generate two versions of the model using slightly different parameter values. For chaotic systems, the outcome of the system is sensitively dependent on the initial conditions in the sense that a slight difference in the initial conditions can result in vastly different outcomes. In view of this, we consider a model to be robust if the sets of all possible outcomes of the two versions of the model are very similar. To illustrate this, consider the simple case in which two very closely related models are used to emulate a physical system in nature. Denote these models as model **A** and model **B**, and if the differences between the two are small, we can regard one as a slightly different version of the other. Some possible differences between models **A** and **B** could be (i) a small change in one of the parameter values, (ii) a slightly different external influence on each, or (iii) a different noise level in the models. Successful modeling requires that the set of all possible outcomes from model **A** agrees closely with the set of all possible outcomes from model **B**. More precisely, model robustness means that for every trajectory of **A**, there exists at least one trajectory of **B** that stays uniformly close to, or shadows, the particular trajectory of **A** and vice versa. Difficulties appear when trajectories from one model fail to be shadowable by trajectories from the other.

The problem becomes critical in the case of unstable dimension variability when there are trajectories of **A** that do not closely follow *any* trajectory of **B** (or vice versa) for all but short periods of time [12]. Because trajectories from the closely related models do not agree, both models are presumably useless in representing the *physical system*. This can be understood by considering a simple ergodic invariant set containing two unstable fixed points: one with a single local unstable direction and one with two local unstable directions [13]. Trajectories wandering in the invariant set can spend arbitrarily long times near each point. Imagine a ball of initial conditions starting near the fixed point with the single unstable direction. Under the dynamics, the complement of the unstable direction is contracting, so the ball of true trajectories will be squeezed into a very thin line along the unstable direction. Due to the model inaccuracy, say, of size ϵ, points on any trajectory $\mathbf{x}_{\text{model}}$ will typically be found a distance ϵ away from all true trajectories. All model trajectories, therefore, lie in a cigarlike tube of size ϵ in the cross section of the tube. When the trajectories visit the neighborhood of the second fixed point with two unstable directions, the small distance between $\mathbf{x}_{\text{model}}$ and all true trajectories will increase exponentially along the *new* unstable direction at a rate determined by the average expanding eigenvalue associated with this direction, as shown schematically in the cross section of the tube in Fig. 1. Thus, whenever this happens, the model trajectories immediately diverge exponentially from the true ones. For a chaotic set with unstable dimension variability, this is by no means a rare phenomenon. In fact, unstable periodic orbits with different numbers of unstable directions are *dense* in the chaotic set, which substantially reduces the time a model trajectory can be expected to remain close to any true trajectory of the natural system.

Qualitatively, the occurrence of an unstable dimension variability in a system of coupled chaotic maps or flows can be seen as follows. Recall that the synchronization manifold $\mathcal{M}$ contains a chaotic attractor, which is identical to that of any individual uncoupled unit. Assume that there is no unstable dimension variability for this attractor and that the

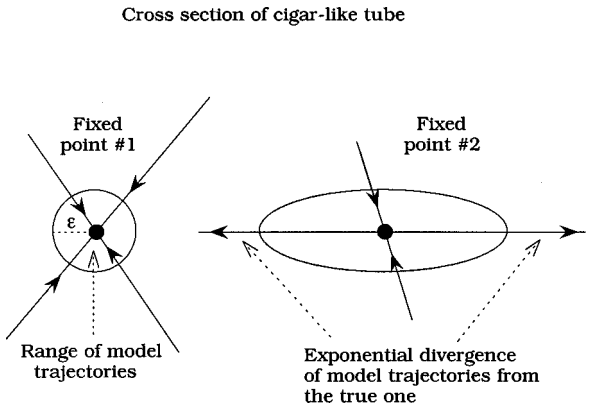

FIG. 1. A schematic illustration of the cross section of the cigar-like tube that characterizes the dynamics of an ergodic set consisting of two fixed points with unstable dimension variability. Divergence between model trajectories and the true one is apparent.

dimension of $\mathcal{M}$ is m. Coupling of the N individual elements immediately introduces an additional $m(N-1)$ dimensional tangent subspace which is *transverse* to $\mathcal{M}$. For zero coupling strength, there is no problem, but as the coupling is turned on, some of the unstable periodic orbits in $\mathcal{M}$ will lose or gain stable transverse directions. Since there are an infinite number of unstable periodic orbits, differing among themselves in the number of local transversely unstable directions, we encounter an unstable dimension variability.

We now argue that an unstable dimension variability can occur even when ϵ is small by examining the stability of the unstable periodic orbits embedded in the synchronization manifold. The variational equation for the model in Eq. (1) is

$$\delta\mathbf{x}_{n+1}^{i}=\mathbf{DF}(\mathbf{x}_{n}^{i})\cdot\delta\mathbf{x}_{n}^{i}-\frac{\epsilon}{2}\sum_{j=1}^{N}G_{ij}\mathbf{DH}(\mathbf{x}_{n}^{i})\cdot\delta\mathbf{x}_{n}^{j}, \tag{3}$$

where **DF** and **DH** denote the derivatives. On $\mathcal{M}$, where $\mathbf{x}^1=\cdots=\mathbf{x}^N=\mathbf{x}$, this can be written concisely as

$$\delta\mathbf{X}_{n+1}=\left(\mathbf{I}_N\otimes\mathbf{DF}(\mathbf{x})-\frac{\epsilon}{2}\mathbf{G}\otimes\mathbf{DH}(\mathbf{x})\right)\cdot\delta\mathbf{X}_{n}, \tag{4}$$

where $\delta\mathbf{X}=(\delta\mathbf{x}^1,\ldots,\delta\mathbf{x}^N)^T$, and $\mathbf{I}_N$ denotes the $N\times N$ identity matrix. If $\mathbf{G}=\mathbf{T}^{-1}\mathbf{\Gamma}\mathbf{T}$ with $\mathbf{\Gamma}=\mathrm{diag}(\gamma_0,\ldots,\gamma_{N-1})$, then the system (4) can be decoupled into the block diagonal form

$$\delta\mathbf{Y}_{n+1}=\left(\mathbf{I}_N\otimes\mathbf{DF}(\mathbf{x})-\frac{\epsilon}{2}\mathbf{\Gamma}\otimes\mathbf{DH}(\mathbf{x})\right)\cdot\delta\mathbf{Y}_{n}, \tag{5}$$

where $\delta\mathbf{Y}=(\delta\mathbf{y}^1,\ldots,\delta\mathbf{y}^N)^T$ and $\delta\mathbf{y}^i=\Sigma_j T_j^i\delta\mathbf{x}^j$. In terms of the individual components, we have N variational equations in $\mathbf{R}^m$:

$$\delta\mathbf{y}_{n+1}^{k}=\left(\mathbf{DF}(\mathbf{x})-\frac{\epsilon}{2}\gamma_k\mathbf{DH}(\mathbf{x})\right)\cdot\delta\mathbf{y}_{n}^{k},\quad k=0,1,\ldots,N-1. \tag{6}$$

Note that the condition $\Sigma_j G_{ij}=0$ implies that G has at least one zero eigenvalue, which we take to be γ_0; the corresponding equation quantifies the stability of an orbit in $\mathcal{M}$. The remaining $N-1$ equations determine the stability of the orbit in the $m(N-1)$ directions *transverse* to $\mathcal{M}$. Let $(\mathbf{x}_1,\mathbf{x}_2,\ldots,\mathbf{x}_p)$ be an orbit of period p in $\mathcal{M}$ whose stability in the kth m plane is determined by the magnitudes of the eigenvalues of the following matrix product:

$$\prod_{i=1}^{p}\left(\mathbf{DF}(\mathbf{x}_i)-\frac{\epsilon}{2}\gamma_k\mathbf{DH}(\mathbf{x}_i)\right),\quad k=0,1,\ldots,N-1. \tag{7}$$

In the transverse subspaces, typically $\gamma_k\neq 0$ so that a finite ϵ causes a shift in the spectrum of this product. Consider all the orbits of period p embedded in the chaotic attractor in $\mathcal{M}$, where p is large. The distribution of the largest Lyapunov exponent of these orbits has a finite width and is centered at λ (independent of the period), where $\lambda>0$ is the Lyapunov exponent of the chaotic attractor. Suppose there is a subset of periodic orbits for which the eigenvalues are just outside the unit circle. For these orbits, when $\epsilon\gtrsim 0$, one or more of the eigenvalues can cross the unit circle inward and lead to the loss of some unstable directions. Similarly, eigenvalues just inside the unit circle can move outward leading to an increase in unstable directions. Unstable dimension variability can thus arise for $\epsilon\gtrsim 0$ when there are unstable periodic orbits with Lyapunov exponents near zero embedded in the chaotic attractor of each individual element. In the next section, we shall see that this behavior does indeed occur, even in the simplest case of two coupled chaotic maps.

III. SYSTEM OF TWO COUPLED HÉNON MAPS

As an illustrative example, we investigate the following system of two coupled Hénon maps [11]:

$$\begin{aligned}
x_{n+1}&=a-x_n^2+by_n+\epsilon(x_n-u_n),\\
y_{n+1}&=x_n,\\
u_{n+1}&=a-u_n^2+bv_n+\epsilon(u_n-x_n),\\
v_{n+1}&=u_n,
\end{aligned} \tag{8}$$

where $\{x,y\}$ and $\{u,v\}$ are the dynamical variables of the two Hénon maps, respectively, a and b are the parameters of the Hénon map, and ϵ is the coupling parameter. The synchronization manifold $\mathcal{M}$ is the plane given by $x=u$ and $y=v$ and the transverse subspace is likewise two-dimensional. We choose $a=1.4$ and $b=0.3$, a parameter setting for which it is believed that the Hénon map possesses a chaotic attractor. This attractor is then the one embedded in $\mathcal{M}$. Unstable periodic orbits of the Hénon map can be computed by using the algorithm in Ref. [14]. Explicit demonstration of unstable dimension variability for the coupled system Eq. (8) then becomes possible.

We can characterize the transverse stability of a typical chaotic trajectory in $\mathcal{M}$ by following the evolution of a small connecting vector $\delta\mathbf{z}$, which is transverse to $\mathcal{M}$. Under the dynamics, this vector can either grow or shrink, depending on whether the synchronization manifold is transversely unstable or stable. Typically, we expect, at time t, the following:

$$|\delta\mathbf{z}(t)|\approx\exp(t\lambda_T)|\delta\mathbf{z}(0)|, \tag{9}$$

where λ_T is the transverse Lyapunov exponent. If $\lambda_T>0$, then $\mathcal{M}$ is unstable and the two coupled maps cannot be synchronized.

Since Eq. (8) only involves two coupled maps, the Jacobian matrix in the eigenspace transverse to the synchronization manifold can be written down explicitly. Introducing the orthogonal coordinates

$$\eta=\frac{1}{\sqrt{2}}(x+u),\quad \sigma=\frac{1}{\sqrt{2}}(y+v),$$
$$\zeta=\frac{1}{\sqrt{2}}(x-u),\quad \rho=\frac{1}{\sqrt{2}}(y-v), \tag{10}$$

we obtain a coupled map in $(\eta, \sigma, \zeta, \rho)$:

$$(\eta,\sigma,\zeta,\rho)_{n+1}=\mathbf{F}(\eta_n,\sigma_n,\zeta_n,\rho_n),$$

where

$$\mathbf{F}=\frac{1}{\sqrt{2}}\begin{pmatrix} 2a-(\zeta^2+\eta^2)+\sqrt{2}b\sigma \\ \sqrt{2}\eta \\ -2\zeta\eta+\sqrt{2}b\rho+2\sqrt{2}\epsilon\zeta \\ \sqrt{2}\zeta \end{pmatrix}. \tag{11}$$

In Eq. (11), ζ and ρ are the dynamical variables in the transverse subspace, so the synchronization manifold is given by $\zeta=\rho=0$. Thus, the Jacobian matrix governing the transverse evolution along an orbit is given by the 2×2 block,

$$\mathbf{DF}_T=\frac{1}{\sqrt{2}}\begin{pmatrix} -2\eta+2\sqrt{2}\epsilon & \sqrt{2}b \\ \sqrt{2} & 0 \end{pmatrix}=\begin{pmatrix} -2x+2\epsilon & b \\ 1 & 0 \end{pmatrix}. \tag{12}$$

Note that $\mathbf{DF}_T$ is independent of ζ and ρ. In numerical experiments, we choose a random unit vector $\delta\mathbf{v}$ in the transverse subspace:

$$\delta\mathbf{v}=\frac{1}{\sqrt{2}}\begin{pmatrix}\delta\zeta\\ \delta\rho\end{pmatrix}=\begin{pmatrix}\delta x-\delta u\\ \delta y-\delta v\end{pmatrix},$$

and compute

$$\lambda_T=\lim_{n\to\infty}\frac{1}{n}\ln|\mathbf{DF}_T^n\cdot\delta\mathbf{v}|,$$

the largest transverse Lyapunov exponent.

When there is no coupling ($\epsilon=0$), $\mathbf{DF}_T$ reduces to the Jacobian matrix of the Hénon map, as expected, and, hence, the transverse Lyapunov exponents are equal to those of the Hénon map. The transverse stability of any periodic orbit embedded in the chaotic attractor restricted to $\mathcal{M}$ can be computed in a similar manner: we simply replace the trajectory by the finite periodic orbit in Eq. (12). Let $\lambda_T^j(p)$ be the largest transverse Lyapunov exponent of the jth periodic orbit of period p. If $\lambda_T^j(p)>0$, this orbit has two unstable directions: one tangent to $\mathcal{M}$ and one transverse to it. However, if $\lambda_T^j(p)<0$, the only unstable direction lies in the synchronization manifold.

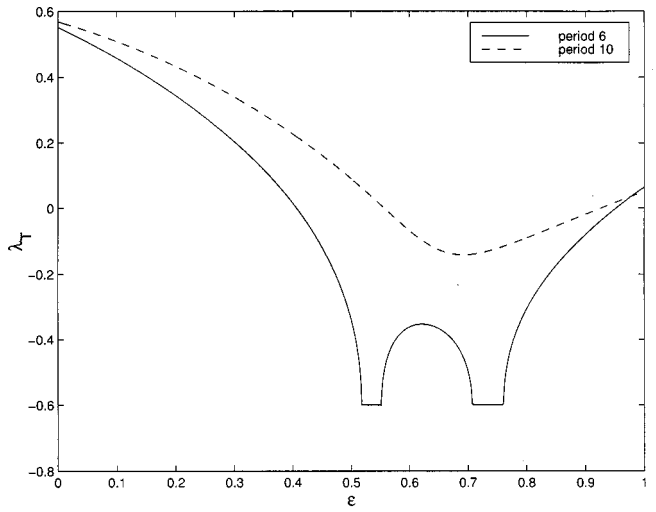

FIG. 2. The largest transverse Lyapunov exponent λ_T vs ϵ for two period-6 orbits and one of the ten period-10 orbits. The flat regions indicate parameter intervals in which the transverse eigenvalues of the orbit become complex.

We can now address the existence of unstable dimension variability in Eq. (8). In the absence of coupling, each periodic orbit has two unstable directions with identical exponents, and the unstable dimension is constant. However, as the coupling parameter ϵ is turned on, unstable dimension variability may occur. To provide evidence for that, we compute the largest transverse Lyapunov exponent for every periodic orbit of up to period 30 as ϵ is systematically increased from zero. Figure 2 shows λ_T versus ϵ for a period-6 orbit and a period-10 orbit, respectively. We see that as ϵ increases up to $\epsilon\approx0.6$, λ_T decreases. An explanation for the flat regions in one of the plots is deferred to Sec. IV. For the jth periodic orbit of period p, the number of unstable dimensions is reduced by one when $\lambda_T^j(p)$ passes through zero at $\epsilon\equiv\epsilon_p^j$ $(j=1,\ldots,N_p)$. The value of ϵ_p^j depends on the period p and also varies from orbit to orbit among the N_p orbits of period p. For a chaotic attractor, typically N_p grows exponentially with p: $N_p\sim e^{h_T p}$, where $h_T>0$ is the topological entropy of the chaotic attractor (≈0.46 in the present case for the attractor in $\mathcal{M}$). Let ϵ_p be the value of the coupling constant at which the first orbit of period p becomes transversely stable. That is, ϵ_p signifies the onset of unstable dimension variability for the orbits of period p: for $\epsilon\gtrsim\epsilon_p$, some of the period-$p$ orbits are transversely stable and therefore have only one unstable direction in $\mathcal{M}$, while others are still transversely unstable and therefore have two unstable directions. To estimate ϵ_p, we compute the distributions of $\lambda_T^j(p)$ at different values of ϵ for all the orbits of period p. Figures 3(a)–3(d) show, for $p=25$, the histograms of $\lambda_T^j(p)$ for all 4498 orbits at $\epsilon=0.0$, 0.5, 1.0, and 1.5, respectively. At $\epsilon=0$, the probability distribution of $\lambda_T^j(p)$ is centered at $\lambda\approx0.42$, the positive Lyapunov exponent of the Hénon attractor. As ϵ increases up to $\epsilon\approx0.6$, the mean of the distribution is translated towards the left and the variance increases. For large values of ϵ (≈0.5) [Fig. 3(b)], a substantial fraction of the period-25 orbits have become transversely stable. This behavior occurs for all periods; another example is given in Figs. 4(a)–4(d), where the distributions of $\lambda_T^j(p)$ for all 16 031 periodic orbits of period 28

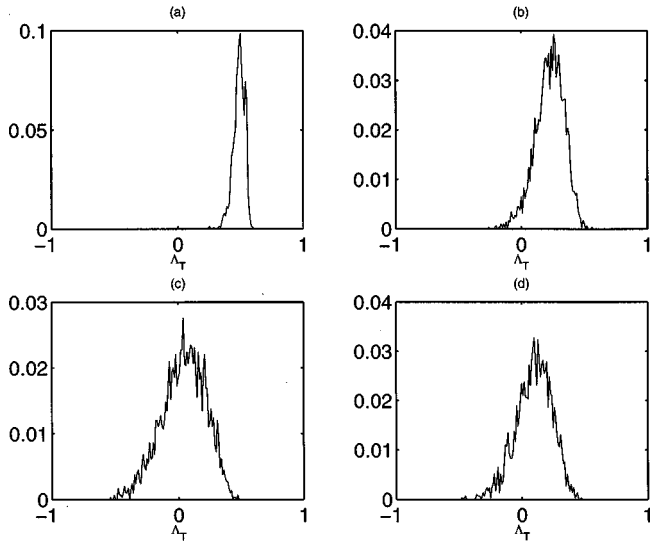

FIG. 3. For $p=25$, the histograms of $\lambda_T^j(p)$ for all 4498 orbits at $\epsilon=0.0$ (a), 0.5 (b), 1.0 (c), and 1.5 (d).

are shown for $\epsilon=0.0$, 0.5, 1.0, and 1.5, respectively.

What is the critical value of ϵ for the onset of unstable dimension variability in Eq. (8)? To address this question, we compute, for each period p up to $p=30$, $\epsilon_{\min}(p)$, which is defined to be the minimum value of ϵ_p *for all periods which are less than or equal to p*, as shown in Fig. 5. We see that for $p=10$, $\epsilon_{\min}(p)\approx 0.051$, but for $p=28$, we have $\epsilon_{\min}(p)\approx 0.002$. The key observation is that $\epsilon_{\min}(p)$ is a *nonincreasing* function of p. (We note that for $p=30$, there are 37 936 unstable periodic orbits, and it was not feasible to carry out the computations for larger values of p.) As $p\to\infty$, it is apparent that $\epsilon_{\min}(p)$ becomes smaller and smaller. This means that the onset of unstable dimension variability may occur at very small values of the coupling parameter.

We now ask, what are some of the dynamical manifestations of unstable dimension variability in coupled systems such as Eq. (8)? To address this, we note that unstable periodic orbits embedded in a chaotic attractor are *atypical* orbits

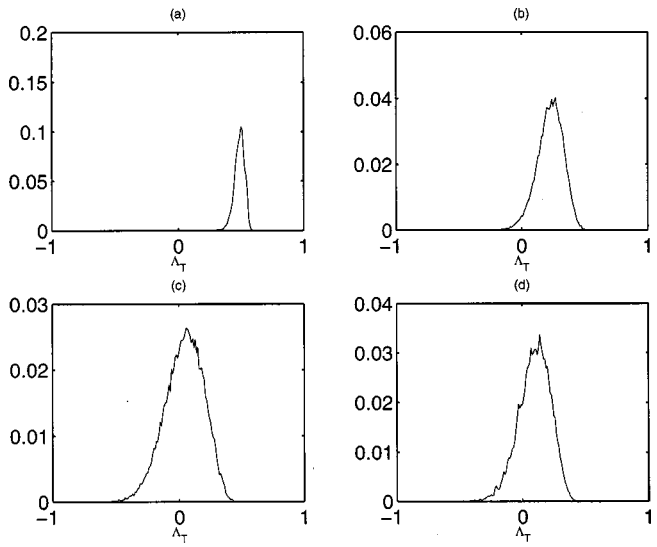

FIG. 4. For $p=28$, the histograms of $\lambda_T^j(p)$ for all 16 031 orbits at $\epsilon=0.0$ (a), 0.5 (b), 1.0 (c), and 1.5 (d).

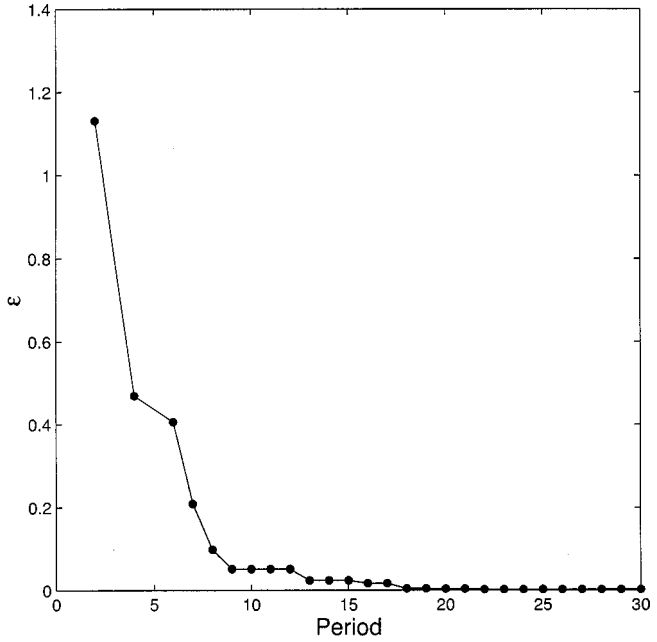

FIG. 5. The minimum value of the coupling strength for the onset of unstable dimension variability for all periodic orbits of period less than or equal to p, $\epsilon_{\min}(p)$, as a function of the p. This function is nonincreasing.

in the sense that they are not traversed by realistic trajectories. What is dynamically accessible to a typical trajectory are the neighborhoods of periodic orbits visited by the trajectory. Let $\mathbf{x}(t)$ be such a trajectory wandering in the chaotic attractor in $\mathcal{M}$, and let λ_T be the largest transverse Lyapunov exponent computed along $\mathbf{x}(t)$. Since unstable periodic orbits are dense in the attractor, $\mathbf{x}(t)$ is arbitrarily close to an infinite number of these orbit components at any time. We therefore expect λ_T to be well approximated by the weighted average of $\lambda_T^j(p)$ when p is large enough so that the N_p orbits of period p are effectively sprinkled over the entire chaotic attractor. In general, we can write [15]

$$\lambda_T = \lim_{p\to\infty} \sum_{j=1}^{N_p} \mu_j(p)\lambda_T^j(p), \tag{13}$$

where $\mu_j(p)$ is the weight, or the natural measure, associated with the jth periodic orbit of period p. In Ref. [15], an approximate formula for $\mu_j(p)$ is given by

$$\mu_j(p) \equiv \frac{1/L_j^1(p)}{\sum_{k=1}^{N_p}[1/L_k^1(p)]}, \tag{14}$$

where $L_j^1(p)$ is the largest eigenvalue of the jth period-p orbit. From Eq. (13), we see that for a system of coupled chaotic oscillators, as the coupling constant ϵ increases from zero, λ_T must decrease from its value at $\epsilon=0$ (the largest Lyapunov exponent of the chaotic attractor in the synchronization manifold) because for all p, and particularly for larger values of p, the distribution of $\lambda_T^j(p)$ is translated towards the left (Figs. 3 and 4) as ϵ increases up to $\epsilon\approx 0.8$. This behavior is shown in Fig. 6, where λ_T versus ϵ is plotted for Eq. (8). To obtain Fig. 6, the transverse Lyapunov exponent

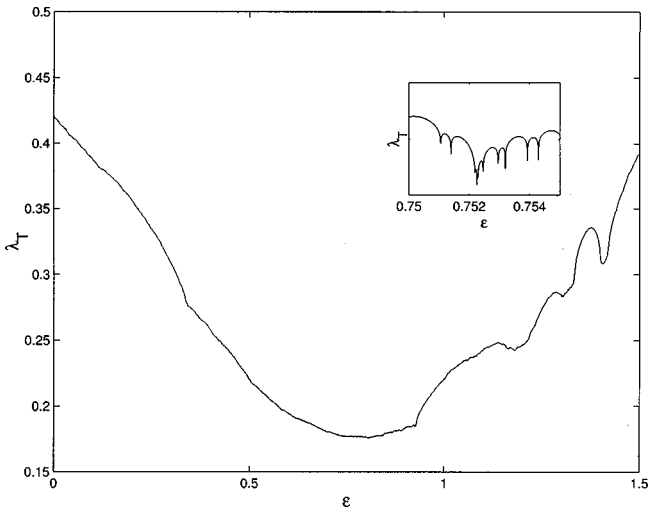

FIG. 6. For Eq. (8), the largest transverse Lyapunov exponent λ_T of a typical trajectory in the chaotic attractor vs the coupling parameter ϵ. We see that the slope of the curve is negative at $\epsilon = 0^+$, meaning that there is a decrease of λ_T as the coupling is turned on. The inset shows a blowup of one portion where we see dips in the plot of λ_T vs ϵ. These dips are due to the occurrence of complex-conjugate transverse eigenvalues occurring for individual periodic orbits.

is computed by using a random trajectory of 10^7 points in the Hénon attractor (with 10^5 iterations of transient time). (The immediate decrease in λ_T as the coupling is turned on is also seen with larger numbers of coupled Hénon maps.) A careful examination of the plot reveals the presence of a large number of dips occurring at various values of ϵ; one of these regions is blown up and displayed in the inset. The origin of these dips can be inferred from the plot of $\lambda_T^j(p)$ versus ϵ for individual periodic orbits such as those in Fig. 2. The dips in $\lambda_T^j(p)$ occur whenever the transverse Lyapunov exponents of the periodic orbit become pairwise degenerate due to the appearance of complex eigenvalues in the transverse spectrum. Because of Eq. (13), a corresponding dip in λ_T occurs when the transverse eigenvalues of some dominant periodic orbits in the sum are complex. This is explained in detail in the next section.

We wish to emphasize that, in order for an unstable dimension variability to be felt by a typical trajectory, it is *not* necessary that λ_T itself be negative, or even close to zero. It is enough that λ_T^p be negative for a nonzero fraction of the periodic orbits of sufficiently long period. A typical trajectory will then visit the neighborhoods of these orbits infinitely often.

The decrease of the transverse Lyapunov exponent as the coupling parameter is increased from zero appears to be a general phenomenon in systems of coupled chaotic oscillators as well. To illustrate this, we have studied the following system of two coupled Rössler [16] oscillators:

$$\dot{x}_{1,2} = -y_{1,2} - z_{1,2} + \epsilon(x_{2,1} - x_{1,2}),$$

$$\dot{y}_{1,2} = x_{1,2} + 0.165 y_{1,2}, \tag{15}$$

$$\dot{z}_{1,2} = 0.2 + z_{1,2}(x_{1,2} - 10.0),$$

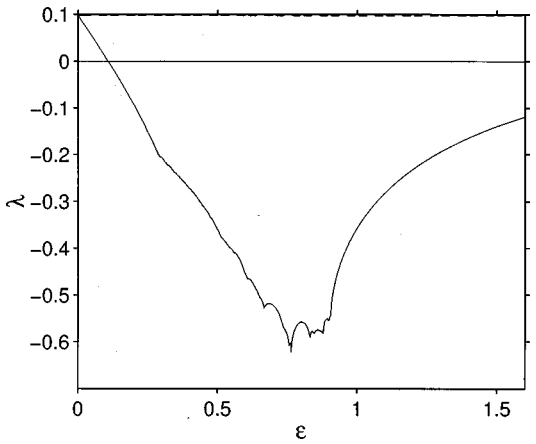

FIG. 7. For the system of two coupled Rössler chaotic oscillators Eq. (15), λ_T vs ϵ. This plot is similar to that in Fig. 6(a).

where in the absence of coupling ($\epsilon = 0$), the two oscillators are chaotic [16]. Introducing the coordinate transformation

$$X = \frac{1}{\sqrt{2}}(x_1 - x_2), \quad \mu = \frac{1}{\sqrt{2}}(x_1 + x_2),$$

$$Y = \frac{1}{\sqrt{2}}(y_1 - y_2), \quad \nu = \frac{1}{\sqrt{2}}(y_1 + y_2), \tag{16}$$

$$Z = \frac{1}{\sqrt{2}}(z_1 - z_2), \quad \rho = \frac{1}{\sqrt{2}}(z_1 + z_2),$$

we obtain orthogonal coordinates in $\mathbf{R}^6$ for which the synchronization manifold $\mathcal{M}$ is given by $X = Y = Z = 0$. At each point of the chaotic attractor in $\mathcal{M}$, the vectors

$$e_1^T = \frac{\partial}{\partial X}, \quad e_2^T = \frac{\partial}{\partial Y}, \quad e_3^T = \frac{\partial}{\partial Z}, \tag{17}$$

form an orthonormal basis for the tangent transverse subspace $T\mathcal{M}^T$. An arbitrarily small vector in the transverse subspace $\delta_T \mathbf{r} \equiv \delta X \mathbf{e}_1^T + \delta Y \mathbf{e}_2^T + \delta Z \mathbf{e}_3^T$ thus evolves according to

$$\frac{d\,\delta_T \mathbf{r}}{dt} = (-2\epsilon\,\delta X - \delta Y - \delta Z)\mathbf{e}_1^T + (\delta X + 0.165\,\delta Y)\mathbf{e}_2^T + [z\,\delta X + (x - 10.0)\,\delta Z]\mathbf{e}_3^T, \tag{18}$$

from which the change in the length of the vector $\delta_T \mathbf{r}$ can be computed, yielding the largest transverse Lyapunov exponent λ_T. Figure 7 shows λ_T versus ϵ for $0 \leqslant \epsilon \leqslant 1.6$. We see that λ_T decreases immediately as the coupling ϵ increases, a behavior also observed for Eq. (8). Thus, we conclude that unstable dimension variability also occurs in Eq. (15) for small ϵ. Note that there is a range of ϵ values where λ_T is actually negative, indicating that the synchronization manifold is transversely stable. Physically, this means that, in the absence of noise, the two chaotic oscillators are synchronized [4].

IV. *N* COUPLED HÉNON MAPS

We now consider a system of N coupled Hénon maps on a circle with periodic boundary conditions:

$$x_{n+1}^i = 1.4 - (x_n^i)^2 + 0.3y_n^i + \frac{\epsilon}{2}(2x_n^i - x_n^{i+1} - x_n^{i-1}),$$
$$y_{n+1}^i = x_n^i, \quad i = 1, \ldots, N, \tag{19}$$

where the coupling is assumed to be nearest-neighbor type. For Eq. (19), the matrices $\mathbf{DF}(\mathbf{x})$, $\mathbf{G}$, and $\mathbf{H}$ of Eq. (4) are given by

$$\mathbf{DF}(\mathbf{x}) = \begin{pmatrix} -2x & b \\ 1 & 0 \end{pmatrix},$$

$$G = \begin{pmatrix} -2 & 1 & 0 & \cdots & 1 \\ 1 & -2 & 1 & \cdots & 0 \\ 0 & 1 & -2 & \cdots & 0 \\ \cdots & \cdots & \cdots & \cdots & \cdots \\ 1 & 0 & 0 & \cdots & -2 \end{pmatrix}_{N\times N},$$

$$\mathbf{H} = \begin{pmatrix} 1 & 0 \\ 0 & 0 \end{pmatrix}. \tag{20}$$

Diagonalization of Eq. (4) in this case gives the following N variational equations in the plane:

$$\delta\mathbf{y}_{n+1}^k = \mathcal{D}_k(\mathbf{x}) \cdot \delta\mathbf{y}_n^k = \begin{pmatrix} -2x - \frac{\epsilon}{2}\gamma_k & b \\ 1 & 0 \end{pmatrix} \cdot \delta\mathbf{y}_n^k,$$
$$k = 0,1, \ldots, N-1. \tag{21}$$

The stability of a period-p orbit lying in $\mathcal{M}$ is determined by the eigenvalues of

$$\mathcal{D}_k^p(\mathbf{x}) = \prod_{i=1}^{p} \begin{pmatrix} -2x_i - \frac{\epsilon}{2}\gamma_k & b \\ 1 & 0 \end{pmatrix}, \quad k = 0,1, \ldots, N-1. \tag{22}$$

We remark on an interesting ''symmetry'' here: the Lyapunov exponents for the periodic orbits in $\mathcal{M}$ occur in pairs which are equidistant and on opposite sides of the point $\alpha = \frac{1}{2}\ln(b)$. This happens because, for each k, the product of the two relevant eigenvalues is equal to $|\det(\mathcal{D}_k^p)| = b^p$ (independent of $\mathbf{x}$). So

$$2\alpha = \frac{1}{p}\ln|\det(\mathcal{D}_k^p)| = \lambda_{1k} + \lambda_{2k}. \tag{23}$$

In particular, the N smallest Lyapunov exponents can be determined by subtracting the N largest from 2α as shown in Fig. 8. The ''flat'' regions seen here and in Fig. 2 for which $\lambda = \alpha$ result from the occurrence of complex eigenvalues in the spectrum of $\mathcal{D}_k^p$. These appear in complex-conjugate pairs with equal moduli, so the corresponding (degenerate) pairs of Lyapunov exponents are necessarily equal to each other and hence to α. Note that, generically, the pair of degenerate Lyapunov exponents remains so over a finite interval.

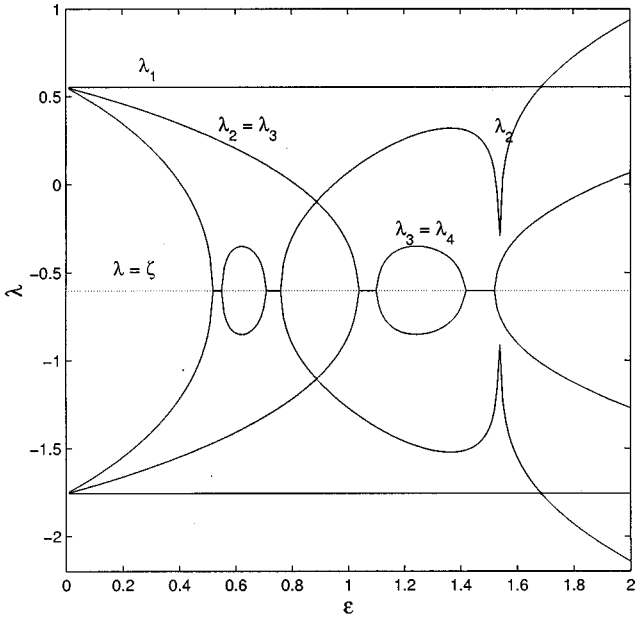

FIG. 8. Lyapunov exponents for $N=4$ coupled Hénon maps along a period-6 orbit as a function of the coupling strength ϵ. Note the symmetry about the line $\epsilon = \alpha$. There are two small ϵ intervals in which this orbit becomes transversely *stable* (i.e., all six transverse Lyapunov exponents are negative).

For illustrative purposes, we have undertaken a series of numerical computations to demonstrate unstable dimension variability in Eq. (19) for $N=5$. The full dynamical system lies in $\mathbf{R}^{10}$ but the invariant synchronization plane is still $\mathbf{R}^2$. We first compute all the orbits of period $\leqslant 28$. We then vary the coupling strength ϵ in the range [0,1.6], and for each chosen value of ϵ in this range we compute the Lyapunov spectrum in each transverse plane for all the unstable periodic orbits. Since $N=5$, when $\epsilon = 0$, each periodic orbit has five degenerate unstable directions with equal eigenvalues. The matrix $\mathbf{G}$ has the following set of eigenvalues for $N=5$: $\gamma_0 = 0$, $\gamma_1 = \gamma_2 = -1.382$, and $\gamma_3 = \gamma_4 = -3.618$. So for ϵ fixed but positive, the Hénon periodic orbits can have five, three, or one unstable directions, corresponding to four, two, or zero transversely unstable directions. Figures 9(a) and 9(b) show the histograms of the largest two transverse Lyapunov exponents ($\lambda_T^1 = \lambda_T^2$) for all orbits of period 28 at $\epsilon = 0.4$ and 0.8, respectively. It can be seen that for $\epsilon = 0.4$, almost all orbits of period 28 have at least two transversely unstable directions, while for $\epsilon = 0.8$, a small fraction of these orbits are transversely stable. Periodic orbits can also have two or four transversely unstable directions. This is shown in Figs. 9(c) and 9(d), where the histograms of the third and the fourth largest transverse Lyapunov exponents ($\lambda_T^3 = \lambda_T^4$) of all period-28 orbits are shown for $\epsilon = 0.4$ and 0.8, respectively. We see that for $\epsilon = 0.4$, a substantial fraction of orbits have negative values of λ_T^3 and λ_T^4, indicating that these orbits can have at most two transversely unstable directions. For $\epsilon = 0.8$, a large fraction of the period-28 orbits have a similar behavior. These results thus clearly indicate

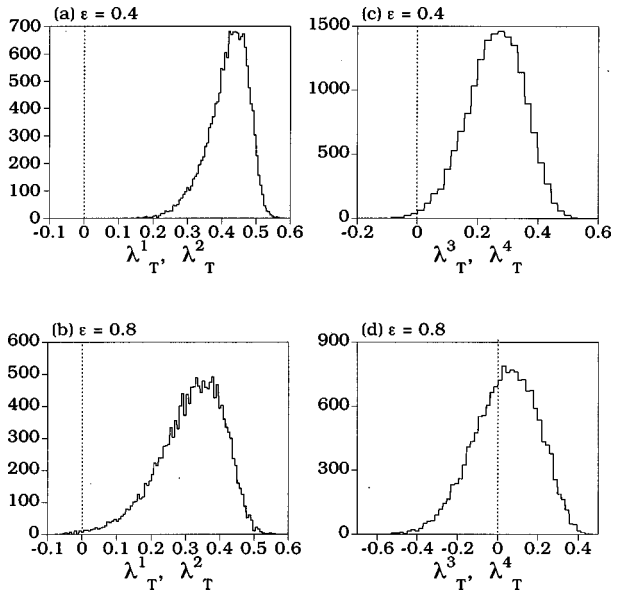

FIG. 9. For $N=5$, $a=1.4$, and $b=0.3$ in Eq. (19): (a) and (b) histograms of λ_T^1 and λ_T^2 ($\lambda_T^1=\lambda_T^2$) for all periodic orbits of period 28 at $\epsilon=0.4$ and 0.8, respectively; (c) and (d) histograms of λ_T^3 and λ_T^4 ($\lambda_T^3=\lambda_T^4$) for all period-28 orbits for $\epsilon=0.4$ and 0.8, respectively.

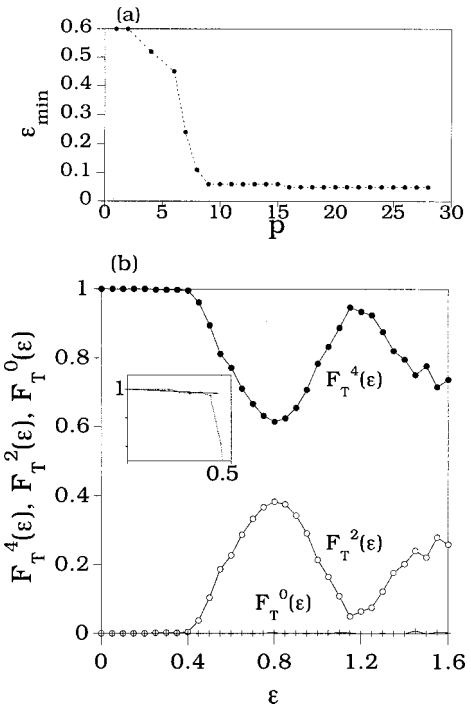

FIG. 10. (a) For $N=5$, $a=1.4$, and $b=0.3$ in Eq. (19), $\epsilon_{\min}$ vs the period p. (b) Fractions of all period-28 orbits with four, two, and zero transversely unstable directions vs ϵ for $0<\epsilon<1.6$. Blow-up in the range $0<\epsilon\leqslant 0.5$ is shown in the inset, which indicates an approximately linear behavior of the fraction near $\epsilon=0$.

unstable dimension variability in Eq. (19) for $\epsilon>0$.

How large must the coupling parameter be for unstable dimension variability to occur? To address this question, we again compute, for a given period p, $\epsilon_{\min}(p)$, the minimum value of the coupling for which unstable dimension variability occurs for *all periodic orbits of period less than or equal to p*, as shown in Fig. 10(a) for $p\leqslant 28$. The function $\epsilon_{\min}(p)$ is a nonincreasing, non-negative function of p, implying that $\epsilon_{\min}$ can be small as $p\to\infty$. This means that unstable dimension variability can occur at small values of the coupling strength. To understand to what extent one encounters unstable dimension variability for periodic orbits of a given (large) period, we compute the fractions of all period-28 orbits which have four, two, and zero transversely unstable directions as functions of ϵ. The results are plotted in Fig. 10(b) for $0\leqslant\epsilon\leqslant 1.6$. The fraction of orbits with four unstable directions decreases linearly as ϵ increased from zero, as shown in the inset of Fig. 10(b) for $0\leqslant\epsilon\leqslant 0.5$. The linear behavior for $\epsilon\gtrsim 0$ can be understood from the histograms shown in Figs. 9(a)–9(d). For small ϵ, almost all period-28 orbits have at least two transversely unstable directions [Fig. 9(a)] and, hence, the fraction of orbits with four transversely unstable directions is proportional to the area of the histograms of λ_T^3 and λ_T^4 on the positive side. This area decreases approximately linearly as the mean of the histogram moves towards the negative side as ϵ increases, and when the center of the histogram is far away from zero. However, for large ϵ, the fraction of orbits with four transversely unstable directions decreases sharply, as the means of the histograms of λ_T^3 and λ_T^4 become close to zero.

Any generic trajectory, which by definition is ergodic with respect to the invariant measure, necessarily comes arbitrarily close to any given periodic orbit infinitely often. Once we have established that a positive fraction of unstable periodic orbits of different dimensionality exist, it follows that a generic trajectory encounters this varying transverse stability as time progresses. For an infinite trajectory, this happens infinitely often of course. The main point here is that, even for small values of the coupling constant, the numerical simulations indicate that there will be an infinite number of UPO's with a number of transversely unstable directions different from the expected number determined by the values of the transverse Lyapunov exponents computed over the trajectory. The consequence is that shadowing is impossible, even for short time intervals.

V. GENERIC ORBITS

Up to this point, we have concentrated on unstable periodic orbits embedded in the invariant synchronization manifold since (a) these do not change with ϵ, so they only need to be computed once, and (b) the subject of synchronization is itself of considerable current interest [4]. However, it is reasonable to ask whether a generic chaotic orbit embedded in the *full* attractor will also encounter unstable dimension variability. Briefly, the answer is that essentially the same reasoning applies.

Consider the case of n coupled chaotic maps with $\epsilon=0$ initially. If $\mathcal{A}$ is the single attractor in $\mathbf{R}^m$, the attractor for the uncoupled system in $\mathbf{R}^{mn}$ is just $\mathcal{A}\times\cdots\times\mathcal{A}$ (n times). If there are N_p orbits of period p in $\mathcal{A}$, then there are roughly $p^{n-1}(N_p)^n$ period-p orbits on the attractor in $\mathbf{R}^{mn}$. Now let $\mathbf{F}_\epsilon(\mathbf{x})$ be the coupled map on $\mathbf{R}^{mn}$. A standard argument using the implicit function theorem shows that if $\mathbf{x}_0$ is an isolated fixed point of $\mathbf{F}_\epsilon^p$ (i.e., a point of period p) when $\epsilon=0$, then there is an interval of width $\delta_{\mathbf{x}_0}$ about $\epsilon=0$ for

which $\mathbf{F}_\epsilon^p$ has a corresponding isolated fixed point $\mathbf{x}_\epsilon$; moreover, if $\mathbf{x}_0$ is hyperbolic, so is $\mathbf{x}_\epsilon$.

So, except at nongeneric points where the matrix $\mathbf{DF}_\epsilon^p - \mathbf{I}$ is singular, each periodic orbit persists for some finite interval about $\epsilon = 0$. However, there are infinitely many such periodic orbits, and it is again the case that $\liminf(\delta_{\mathbf{x}_0}) = 0$. That is, once again, for a typical orbit on the attractor we would expect to encounter unstable dimension variability as soon as the coupling is turned on. If the global attractor persists for sufficiently large values of ϵ, severe modeling difficulties can be expected.

In fact, a generic orbit on the attractor of the full set of coupled maps will be ergodic with respect to the natural measure; hence it will approach the synchronization manifold arbitrarily closely an infinite number of times, with the result that unstable dimension variability on the synchronization manifold implies its existence on the full attractor.

VI. DISCUSSION

Scientists and engineers rely heavily on quantitative models to understand natural phenomena and technological systems. Usually, for a particular process, data from laboratory experiments or from observations are analyzed and, together with physical laws, a model of the process is formulated. The models are then used to understand the particular process, to make predictions, and to control its dynamics. An important class of models consists of *deterministic* dynamical systems in which the relevant physical variables evolve in time according to a set of prescribed rules. A natural question is then to what extent predictions from a deterministic model are expected to be valid. This is particularly germane when the system is chaotic, that is, when the system has a sensitive dependence on initial conditions. Previous work has suggested [17] that there is a hierarchy of levels of dynamical difficulties with deterministic modeling. (i) *Minor modeling difficulties*: hyperbolic chaotic systems exhibiting a sensitive dependence on initial conditions. For these systems, trajectories of a model can always be shadowed by trajectories of the natural system for an infinite time [18]. (ii) *Moderate modeling difficulties*: chaotic systems with nonhyperbolic tangencies. For these systems, trajectories of a model are shadowed by trajectories of the natural system for a long but finite amount of time [19]. (iii) *Severe modeling difficulties*: nonhyperbolic chaotic systems with unstable-dimension variability [6–8,20]. For these systems, the model shadowing times are surprisingly short [12].

The principal result of this paper is that unstable dimension variability occurs in systems of coupled chaotic maps and flows, and that therefore these systems exhibit severe modeling difficulties. We have given theoretical justification and numerical evidence for the occurrence of unstable dimension variability in these systems, and argued that it can occur at small values of the coupling parameters. We expect these results to be general for coupled systems since the existence of chaotic dynamics and synchronization manifold is typical in such systems. Finally, it is possible that our results may shed some light on the well-known difficulties of obtaining physically realistic simulations from systems of partial differential equations if they are integrated numerically via a spatial discretization leading to a finite-dimensional dynamical system.

ACKNOWLEDGMENTS

Y.C.L. was supported by AFOSR under Grant No. F49620-98-1-0400, and by NSF under Grants No. PHY-9722156 and No. DMS-962659. C.G. was supported by ONR (Physics Division) and by the CNPq/NSF-INT Program.

[1] There is a large literature on coupled oscillators. Even an abbreviated list of references is prohibitively long. For a list of representative papers in optical, chemical, condensed matter, biological, neural networks, and other systems, see J. F. Heagy, T. L. Carroll, and L. M. Pecora, Phys. Rev. E **50**, 1874 (1994).

[2] P. Hadley, M. R. Beasley, and K. Wiesenfeld, Phys. Rev. B **38**, 8712 (1988); K. Y. Tsang and I. B. Schwartz, Phys. Rev. Lett. **68**, 2265 (1992); S. Nichols and K. Wiesenfeld, Phys. Rev. A **45**, 8430 (1992); S. H. Strogatz and R. E. Mirollo, Phys. Rev. E **47**, 220 (1993); S. Watanabe and S. H. Strogatz, Physica D **74**, 197 (1994); S. Watanabe, H. S. J. van der Zant, S. H. Strogatz, and T. P. Orlando, *ibid.* **97**, 429 (1996).

[3] R. Roy and K. S. Thornburg, Jr., Phys. Rev. Lett. **72**, 2009 (1994).

[4] J. F. Heagy, T. L. Carroll, and L. M. Pecora, Phys. Rev. Lett. **73**, 3528 (1994); J. F. Heagy, L. M. Pecora, and T. L. Carroll, *ibid.* **74**, 4185 (1995); L. M. Pecora and T. L. Carroll, *ibid.* **80**, 2109 (1998)).

[5] Consider the case where two models **A** and **B** are very close to each other, where **B** is a slight perturbation of **A**. Model shadowability occurs if there exist trajectories of model **A** which stay close to a given trajectory of model **B**. See, for example, Ref. [6].

[6] Y.-C. Lai, C. Grebogi, and J. Kurths, Phys. Rev. E **59**, 2907 (1999).

[7] S. P. Dawson, C. Grebogi, T. Sauer, and J. A. Yorke, Phys. Rev. Lett. **73**, 1927 (1994).

[8] E. J. Kostelich, I. Kan, C. Grebogi, E. Ott, and J. A. Yorke, Physica D **109**, 81 (1997).

[9] The dynamics is hyperbolic on a chaotic attractor if at each point of the trajectory the phase space can be split into an expanding subspace and a contracting one and the angle between them is bounded away from zero. Furthermore, the expanding subspace evolves into the expanding one along the trajectory and the same is true for the contracting subspace. Otherwise the set is nonhyperbolic. For hyperbolic chaotic systems, numerical trajectories can be shadowed by true trajectories for an arbitrarily long time [D. V. Anosov, Proc. Steklov Inst. Math. **90**, 1 (1967); R. Bowen, J. Diff. Eqns. **18**, 333 (1975)]. In general, nonhyperbolicity is a complicating feature because it can cause fundamental difficulties in the study of chaotic dynamics, a known one being the shadowability of numerical trajectories by true trajectories [C. Grebogi, S. M.

Hammel, and J. A. Yorke, J. Complexity **3**, 136 (1987); Bull. Am. Math. Soc. **19**, 465 (1988); C. Grebogi, S. M. Hammel, J. A. Yorke, and T. Sauer, Phys. Rev. Lett. **65**, 1527 (1990); T. Sauer and J. A. Yorke, Nonlinearity **4**, 961 (1991)].

[10] Y.-C. Lai and C. Grebogi, Phys. Rev. Lett. **82**, 4803 (1999).

[11] M. Hénon, Commun. Math. Phys. **50**, 69 (1976).

[12] T. Sauer, C. Grebogi, and J. A. Yorke, Phys. Rev. Lett. **79**, 59 (1997).

[13] R. Abraham and S. Smale, Proc. Symp. Pure Math. **14**, 5 (1970).

[14] O. Biham and W. Wenzel, Phys. Rev. Lett. **63**, 819 (1989); Phys. Rev. A **42**, 4639 (1990).

[15] C. Grebogi, E. Ott, and J. A. Yorke, Phys. Rev. A **37**, 1711 (1988); Y.-C. Lai, Y. Nagai, and C. Grebogi, Phys. Rev. Lett. **79**, 649 (1997); Y.-C. Lai, Phys. Rev. E **56**, 6531 (1997).

[16] O. E. Rössler, Z. Naturforsch. A **31**, 1168 (1976).

[17] L. Poon, C. Grebogi, T. Sauer, and J. A. Yorke (unpublished).

[18] D. V. Anosov, Proc. Steklov Inst. Math. **90**, 1 (1967); R. Bowen, J. Diff. Eqns. **18**, 333 (1975).

[19] S. M. Hammel, J. A. Yorke, and C. Grebogi, J. Complexity **3**, 136 (1987); Bull. Am. Math. Soc. **19**, 465 (1988); C. Grebogi, S. M. Hammel, J. A. Yorke, and T. Sauer, Phys. Rev. Lett. **65**, 1527 (1990); T. Sauer and J. A. Yorke, Nonlinearity **4**, 961 (1991).

[20] S. P. Dawson, Phys. Rev. Lett. **76**, 4348 (1996); P. Moresco and S. P. Dawson, Phys. Rev. E **55**, 5350 (1997).